Investigation of Li/Ca variations in aragonitic shells of the ocean quahog Arctica islandica, northeast Iceland

Julien Thébault, Bernd R. Schöne, Nadine Hallmann, Matthias Barth, Elizabeth V. Nunn

Investigation of Li/Ca variations in aragonitic shells of the ocean quahog *Arctica islandica* (northeast Iceland)

Julien Thébault [a,*], Bernd R. Schöne [a], Nadine Hallmann [a], Matthias Barth [b], and Elizabeth V. Nunn [a]

[a] Earth System Science Research Centre (Geocycles), Department of Applied and Analytical Paleontology (INCREMENTS), Institute of Geosciences, University of Mainz, Johann-Joachim-Becherweg 21, 55128 Mainz, Germany

[b] Earth System Science Research Centre (Geocycles), Department of Geochemical Petrology, Institute of Geosciences, University of Mainz, Johann-Joachim-Becherweg 21, 55128 Mainz, Germany

Running title: Li/Ca record in aragonitic bivalve shells

* Correspondence author. Present address: Université de Bretagne Occidentale, Laboratoire des Sciences de l'Environnement Marin (UMR6539 UBO/CNRS/IRD), Institut Universitaire Européen de la Mer, Technopole Brest-Iroise, Place Nicolas Copernic, 29280 Plouzané, France. Phone: +33 2 98 49 86 33; Fax: +33 2 98 49 86 45; Email: julien.thebault@univ-brest.fr

1   **ABSTRACT**

2

3   Inter- and intra-annual variations in lithium-to-calcium ratio were investigated with high

4   temporal resolution in the aragonitic outer shell layer of juvenile *Arctica islandica* (Mollusca;

5   Bivalvia) collected alive in 2006 off northeast Iceland. Li/Ca_{shell} ranged between 7.00 and

6   11.12 μmol mol^{-1} and presented well-marked seasonal cycles with minimum values recorded

7   at the annual growth lines; a general pattern was a progressive increase in Li/Ca_{shell} from

8   March to May, followed by a plateau in June, and a decrease down to minimum values in

9   July–August. Li/Ca_{shell} was correlated with $\delta^{18}O_{shell}$-derived temperature but the strength of

10 this relationship was weak ($r^2 < 0.25$; $p < 0.05$). It covaried significantly with microgrowth

11 increment width and with the discharge from one of the closest rivers. Seasonal variations of

12 Li/Ca_{shell} in *A. islandica* may most likely be explained (1) by calcification rate, and/or (2) by

13 significant river inputs of Li-rich silicate particles flowing to the sea as soon as snow melts. In

14 the first case, Li/Ca_{shell} may be a useful proxy for addressing seasonal variations of growth

15 rate in bivalves that lack discernable microgrowth patterns. Abrupt decreases of Li/Ca_{shell} may

16 in turn help identify growth retardations due to harsh environmental conditions. Alternatively,

17 if Li/Ca_{shell} variations are linked to particulate Li inputs by rivers, this could be a new proxy

18 for the intensity of mechanical weathering of Icelandic basalts, with interesting perspectives

19 for the reconstruction of frequency and intensity of past jökulhlaups (subglacial outburst

20 floods). Further works, including experimental studies, are needed to test these hypotheses.

22   **Index Terms:**

23   0424 Biogeosciences: Biosignatures and proxies

24   0438 Biogeosciences: Diel, seasonal, and annual cycles (4227)

25   0454 Biogeosciences: Isotopic composition and chemistry (1041, 4870)

26   4870 Oceanography: Biological and chemical: Stable isotopes (0454, 1041)

27   4875 Oceanography: Biological and chemical: Trace elements (0489)

28   **1. INTRODUCTION**

29

30   During the past sixty years, a large number of studies have focused on the use of

31   elemental concentrations in marine sediment cores as proxies for past variations of

32   environmental parameters. These parameters include, among others, temperature (proxies:

33   Mg/Ca, Sr/Ca), alkalinity (Ba/Ca), dissolved inorganic carbon concentration (Cd/Ca), ocean

34   circulation (Cd/Ca, Nd, Hf, Pb), biological productivity ($BaSO_4$, Pa/Th, Be/Th, U) and

35   sedimentation rate (^{230}Th, ^{210}Pb, ^{231}Pa/^{230}Th) (for thorough reviews, see: Wefer et al., 1999;

36   Henderson, 2002). However, the temporal resolution of such paleoceanographic

37   reconstructions is low, generally coarser than decades. Therefore, efforts have been made to

38   assess the potential of elemental content in marine biogenic carbonates, especially bivalve

39   mollusk shells, as high-resolution proxies for environmental conditions (e.g. Stecher et al.,

40   1996; Vander Putten et al., 2000; Thébault et al., 2009).

41   Bivalve shells grow by accretion of calcium carbonate crystals, either in the form of

42   calcite, aragonite, or both depending on the species (Pannella and MacClintock, 1968). Shell

43   growth, however, does not occur continuously over a day, or over a year; instead, growth

44   ceases periodically, on ultradian (several growth stops during a single day), circatidal (semi-

45   diurnal, ca. 12.4h), circadian (solar day, ca. 24h), circalunidian (lunar day, ca. 24.8h), or

46   annual timescales (Schöne, 2008). These growth stops result in the formation of so-called

47   growth lines, which are enriched in organic matter and separate growth increments that

48   represent equal time slices. These periodic growth lines can therefore be used to assign

49   precise calendar dates to each successive increment of accreted shell material. This

50   characteristic gives bivalve shells an outstanding potential for the high-resolution

51   reconstruction of paleoenvironmental conditions, especially through geochemical analyses.

52   For example, skeletal oxygen isotope composition (δ^{18}O) of many bivalve species (including

53   scallops, mussels, and clams) has been extensively used since the pioneering work of Epstein

54   et al. (1953) to infer paleotemperature variations, sometimes with an accuracy of less than

55   1°C (Chauvaud et al., 2005; Thébault et al., 2007).

56   In the past decade, the elemental composition of bivalve shells has also been

57   increasingly used for paleoenvironmental reconstructions. Bivalve shells are not exclusively

58   made of $CaCO_3$. Aside from Ca, a number of minor and trace elements are also incorporated

59   within the shell during its formation, either in an interstitial location within the crystal lattice

60   or as carbonates (substitution for Ca^{2+}; Okumura and Kitano, 1986), or even within the

61   organic matrix (Lingard et al., 1992), which can represent up to 5% of the shell dry weight

62   (Marin and Luquet, 2004). The incorporation of these elements is known to be partly

63   controlled by various environmental parameters, either physical (temperature, salinity),

64   chemical (seawater elemental concentration, metallic contamination), or biological (primary

65   production). Physiology, however, also exerts an important control on the chemical

66   composition of bivalve shells (Schöne, 2008).

67   Micro-analytical techniques (e.g. laser ablation coupled to an ICP-MS system = LA-

68   ICP-MS; Craig et al., 2000) allow the accurate measurement of tens of elements archived in

69   biogenic carbonates within a few seconds. Their abiding improvement considerably increases

70   the probability of discovering new paleoenvironmental proxies. With the exception of a few

71   studies (e.g. Lindh et al., 1988; Carriker et al., 1996; Dick et al., 2007) however, most

72   investigations on the geochemical composition of bivalve shells have only dealt with a few

73   elements (mainly Sr, Mg, Ba, and some trace metals including Mn, Pb, Zn, and Cd).

74   Lithium is a trace element that (1) is easily measurable using mass spectrometers, (2)

75   has been demonstrated to present an interesting potential as a paleoceanographic proxy in

76   some marine biogenic carbonates (Delaney et al., 1985; Delaney et al., 1989; Hall and Chan,

77   2004; Marriott et al., 2004a,b; Hathorne and James, 2006; Montagna et al., 2006), and (3) has

78   surprisingly not yet been analyzed in bivalve shells. One of the first studies dealing with

79   Li/Ca ratios in marine biogenic carbonates suggested that this ratio in foraminiferal calcite

80   was partly controlled by the Li/Ca ratio of the growing medium (Delaney et al., 1985). This

81   was later confirmed by Hathorne and James (2006) who demonstrated that Li/Ca in

82   foraminifera could be used to reconstruct past changes in the Li/Ca ratio of seawater, which

83   could be interpreted in terms of continental silicate weathering rate. Several studies have also

84   highlighted significant inverse relationships between temperature and Li/Ca in foraminifera

85   (Hall and Chan, 2004; Marriott et al., 2004a), in calcitic brachiopods (Delaney et al., 1989), in

86   coralline aragonite (Marriott et al., 2004b; Montagna et al., 2006), and in inorganic calcite

87   (Marriott et al., 2004b). It has finally been suggested that the main factor controlling Li

88   incorporation in foraminifera is not temperature but calcification rate (Hall and Chan, 2004;

89   Marriott et al, 2004a). Because calcification rate may be a function of CO_3^{2-} concentration in

90   the oceans, it has been suggested that the Li/Ca ratio in foraminifera could be a potential

91   proxy of past atmospheric CO_2 (Hall and Chan, 2004).

92   Here, we present for the first time Li/Ca records in bivalve mollusk shells. We have

93   focused on juvenile ocean quahogs *Arctica islandica* (Linnaeus, 1767) collected alive in 2006

94   off the coast of northeast Iceland, probably one of the last pristine ecosystems in the North

95   Atlantic. *A. islandica* has all the characteristics necessary for paleoceanographic

96   reconstructions. First, it produces circadian and annual growth patterns in its aragonitic shell

97   (Schöne et al., 2005a). Second, it holds the longevity record for bivalves and may in fact be

98   the longest-lived non-colonial animal, living up to 4 centuries (Schöne et al., 2005b;

99   Wanamaker et al., 2008a). Third, it exhibits a broad biogeographic distribution centered

100   around Iceland, inhabiting the continental shelves on both sides of the North Atlantic, in

101   Europe from the Barents Sea to the Bay of Cadiz in Spain, and in North America from

102   Newfoundland to Cape Hatteras (Thorarinsdóttir and Jacobson, 2005). Fourth, this species has

103   been intensively studied for its anatomy, behavior, physiology, biology, and ecology

104   (Witbaard, 1997). And finally, several studies have already highlighted that shells of

105   *A. islandica* provide multi-proxy records of environmental variables. Changes in

106   environmental parameters are recorded in variations of growth rates (Marchitto et al., 2000;

107   Schöne et al., 2003; Schöne et al., 2005b), stable isotope composition (Weidman et al., 1994;

108   Schöne et al., 2004; Schöne et al., 2005a,b,c; Wanamaker et al., 2008b) and trace element

109   concentrations (Epplé, 2004; Toland et al., 2000; Liehr et al., 2005).

110   The aims of this paper are (1) to analyze the behavior of Li/Ca in *A. islandica* aragonitic

111   shells (inter- and intra-annual variability) using variations of the oxygen isotope composition

112   of these shells as chronological checks, (2) to review the different processes that may explain

113   the temporal variations of this ratio, and (3) to assess if Li/Ca could be a promising addition to

114   the arsenal of proxies already used in bivalve shells.

115

116   **2. MATERIAL AND METHODS**

117

118   **2.1. Study area**

119   Our study site is located in Þistilfjörður (northeast Iceland; 66°10.751'N –

120   15°21.296'W), 1 km off the southwestern edge of Langanes Peninsula and 3 km away from

121   Hafralónsá estuary (Fig. 1). Hafralónsá and Sandá are the two main rivers flowing into

122   Þistilfjörður. Catchments of these two non-glacial rivers are comprised of old basaltic rocks

123   (> 3.1 million years of age). Water depth at our study site is 30 m and the substrate mainly

124   consists of sand and silt sediments. Hydrographic conditions off north Iceland largely depend

125   on the physical characteristics of the East Icelandic Current, which in turn depend on the

126   eastward transport of Greenland Polar Water by the East Greenland Current and the

127   northward transport of Irminger Atlantic Water by the North Irminger Current (Hopkins,

128   1991). No environmental survey has ever been conducted in Þistilfjörður because of its

129   isolated situation in this remote part of Iceland. The closest site where environmental data are

130   available is located 50 km northeastward of our study site, off the northeastern part of the

131   Langanes Peninsula (Langanes Austur LA1, 66°22'N – 14°22'W; Fig. 1). Environmental

132   conditions at LA1 are also mainly controlled by the relative intensities of the East Icelandic

133   Current and the North Irminger Current. Temperature and salinity are measured at this

134   location at a depth of 20 m by the Oceanographic Group of the Marine Research Institute of

135   Reykjavik using a CTD profiler (data available at http://www.hafro.is/Sjora/). This dataset

136   indicates that water temperature is lowest in February–March (mean [2000-2006] = 2.8°C; σ

137   = 0.9°C) and reaches a maximum in August (7.9°C; σ = 0.8°C). Over the same period, salinity

138   variations ranged between 34.4 and 34.8. These temperature and salinity values are similar to

139   those measured at 20-30 m water-depth in two other fjords in North Iceland: Reykjarfjörður

140   (Andrews et al., 2001) and Ísafjörður (Assthorsson, 1990). From early May to the end of

141   August, somewhat lower salinities (< 34) can be observed near the surface in Icelandic fjords

142   because of meltwater runoff from the land. However, these low salinities are restricted to the

143   top 10 m of the water column (Assthorsson, 1990; Andrews et al., 2001). Therefore,

144   temperature and salinity data measured at 20 m depth at LA1 likely reflect those of our study

145   site at 30 m depth.

146   The seawater oxygen isotope composition of our study site was measured on 17th

147   August 2006 ($\delta^{18}O_{water}$ = − 0.58 ‰ VSMOW; Salinity = 34.58). Seasonal variations in

148    $\delta^{18}O_{water}$ are expected given the salinity variations around the Langanes Peninsula but

149   coefficients of the local $\delta^{18}O_{water}$–salinity relationship are unknown. The $\delta^{18}O_{water}$ and salinity

150   values were measured off northwest Iceland in October 1998 (65.98–68.72°N; 22.98–

151   29.25°W; depth = 10-30 m) in the framework of the VEINS Program (Variability of

152   Exchanges In the Northern Seas; data compiled by Schmidt et al., 1999). These data indicate

153   that, over the salinity range 32-35, we can expect a lowering of the $\delta^{18}O_{water}$ values of 0.68 ‰

154   for every unit decrease in salinity. Given (1) $\delta^{18}O_{water}$ and salinity values measured on

155   17/08/2006 at our study site, and (2) the slope of the $\delta^{18}O_{water}$–salinity relationship derived

156   from the VEINS Program, we can expect seasonal variations of $\delta^{18}O_{water}$ at our study site of

157   between $-$ 0.7 and $-$ 0.4 ‰ VSMOW over the salinity range 34.4-34.8.

158

159   **2.2. Shell sampling and preparation**

160   Two specimens of *Arctica islandica* were collected alive on 17 August 2006 by

161   dredging on our study site in Þistilfjörður, at a depth of 30 m. Both specimens (ICE06-6.2-

162   A55 and ICE06-6.2-A56, hereafter simply named A55 and A56) were juveniles with a shell

163   height of 33.0 and 31.2 mm, respectively (shell length of 40.0 and 37.4 mm, respectively; Fig.

164   2a). We chose young specimens because *A. islandica* grows fairly rapidly during early

165   ontogenetic stages (Jones, 1983; Weidman et al., 1994; Jones, 1998; Kilada et al., 2007) and

166   young shells therefore provide the highest temporal resolution in carbonate records.

167   Immediately after dredging, the soft parts were discarded and the right and left valves

168   kept frozen until analysis. The left valves of shells A55 and A56 were gently rinsed with de-

169   ionized water and air-dried. Each valve was mounted on a Plexiglas cube using a two-part

170   methacrylat glue (plastic welder, Gluetec GmbH & Co. KG, Germany) and embedded in a

171   two-part metal-epoxy resin (Wiko, Germany) to strengthen the shell and to avoid shell

172   fracture during sawing (Fig. 2b). Two immediately adjacent, 2.6-mm-thick sections were cut

173   from each valve perpendicular to the growth lines along the axis of maximum growth using a

174   low-speed precision saw (Isomet 1000, Buehler Ltd., IL, USA) equipped with a 0.4 mm thick

175   diamond-coated blade cooled and kept wet using de-ionized water (Fig. 2c). These

176   "mirroring" sections were then mounted on glass slides, manually ground with ca. 12 µm and

177   8 µm SiC powder, and polished with 1 µm Al_2O_3 powder to visualize the internal growth

178   patterns. Thick sections were ultrasonically rinsed with de-ionized water between each

179   grinding/polishing step to remove any adhering grinding powder. Thick section "A" was used

180   for isotopic analyses and thick section "B" for trace elemental analyses. Once geochemical

181   analyses were done, these thick sections were cleaned with ethanol before being etched in the

182   so-called Mutvei's solution for 25 minutes at 37-40°C in order to resolve inter- and intra-

183   annual growth lines and increments (see Schöne et al. (2005d) for a detailed description of

184   this method). Finally, the sections were gently rinsed with de-ionized water and air-dried.

185   Microgrowth increment width was subsequently measured using the image analysis software

186   Panopea (© 2004 Peinl and Schöne). High-resolution photographs of these four sections were

187   taken using a Nikon Coolpix 995 digital camera attached to a Wild Heerbrugg M3Z

188   stereozoom microscope. Photo stitching software (Photoshop Elements 2.0) was then used to

189   assemble the 25-30 photographs taken for each section into a single, high-resolution picture.

190

191   **2.3. Isotopic analyses**

192   The oxygen isotope ratio ($^{18}O/^{16}O$) of marine biogenic carbonate is controlled by

193   temperature and the oxygen isotope composition of the seawater from which it precipitates

194   (McCrea, 1950; Epstein et al., 1953). Therefore, shells of our two *A. islandica* specimens

195   were sampled for isotopic analyses in order to reconstruct variations in the bottom-water

196   temperatures these animals experienced during their life. Aragonite samples (48 and 50

197   samples on shells A55 and A56 respectively) were collected in thick sections "A" using a

198   micro-drill (Minimo C121, Minitor Co. Ltd., Japan) equipped with a 0.3 mm tungsten carbide

199   drill bit (model H52.104.003, Gebr. Brasseler GmbH & Co. KG, Germany). Samples were

200   taken in the outer shell layer along an axis running from the ventral margin and toward the

201   youth portions of the shells. Holes drilled in these sections were ca. 350 μm in diameter.

202   Aliquots of shell aragonite weighing between 38 and 125 μg (mean = 80 μg) were analyzed at

203   the University of Frankfurt using an automated Gas Bench II carbonate device interfaced with

204   a Thermo Finnigan MAT 253 isotope ratio mass spectrometer. Shell isotopic data are

205   expressed in conventional delta (δ) notation (Epstein et al., 1953) relative to the VPDB

206   standard. The in-house standard used was a Carrara marble ($\delta^{18}O_{Carrara} = -1.74$ ‰ VPDB)

207   calibrated against NBS19. The isotopic value used for this calibration was $\delta^{18}O_{NBS19} = -2.20$

208   ‰ VPDB (for more details, see Fiebig et al., 2005). Repeated analyses of this standard

209   yielded a reproducibility (1σ) of 0.07 ‰ VPDB.

210   To temporally align aragonite samples taken between two annual growth lines, we

211   compared the temperature reconstructed from our $\delta^{18}O_{shell}$ records (hereafter referred as $T_{\delta18O}$)

212   with seasonal variations of seawater temperature measured at 20 m depth at station LA1. To

213   this end, we used the empirically determined paleothermometry equation of Grossman and Ku

214   (1986; equation 1 in their paper). A modification of this equation was, however, required as

215   their water values were reported in VSMOW minus 0.27 ‰ (Hut, 1987). Once corrected, their

216   equation translates to:

217

218          $$T_{\delta18O} = 19.43 - 4.34\,(\delta^{18}O_{shell} - \delta^{18}O_{water}) \qquad \text{(Eq. 1)}$$

219

220   where $T_{\delta18O}$ is seawater temperature (in °C) reconstructed from $\delta^{18}O_{shell}$, and $\delta^{18}O_{shell}$ and

221     $\delta^{18}O_{water}$ are the oxygen isotope composition of aragonite and water expressed in ‰ relative to

222   the VPDB and VSMOW standards respectively. We used an average $\delta^{18}O_{water}$ value of -0.55

223   ‰ VSMOW. In order to estimate the uncertainty on $T_{\delta18O}$, i.e. half the difference between

224   upper and lower bounds, we applied the following formula using (1) the uncertainty in

225     $\delta^{18}O_{shell}$ value given by IR-MS ($\varepsilon_{IRMS} = \pm0.07$ ‰), and (2) the estimated range of $\delta^{18}O_{water}$

226   (min. $= -0.7$ ‰ ; max. $= -0.4$ ‰):

227

228    $$\text{Uncertainty} = 4.34 \times (2 \, \varepsilon_{IRMS} + \delta^{18}O_{water \, max.} - \delta^{18}O_{water \, min.}) / 2 \quad \text{(Eq. 2)}$$

229

230   This resulted in an absolute uncertainty on $T_{\delta 18O}$ of $\pm 0.95°C$.

231

232   **2.4. Li/Ca$_{shell}$ analyses**

233   Li/Ca ratios were analyzed in thick sections "B" using LA-ICP-MS at the University of

234   Mainz. An Agilent 7500ce quadrupole ICP-MS (Agilent Technologies Inc., CA, USA)

235   coupled to a UP-213 laser ablation system (New Wave Research, CA, USA) was used with

236   the parameters listed in Table 1. Aragonite samples ($n = 332$ in each shell) were ablated in the

237   outer shell layer from the ventral margin toward the youth portions of the shells at a constant

238   distance from the shell surface (400 μm). The diameter of the laser spots was 80 μm and the

239   distance between the centers of two successive spots was 100 μm (i.e. 20 μm between edges

240   of two successive spots). During acquisition, signal intensities were recorded for ^{7}Li, ^{43}Ca and

241   ^{44}Ca. The intensity of the isotope of interest was systematically normalized against the ^{43}Ca

242   signal (internal standard) in order to correct for laser beam energy drift, focus variation at the

243   sample surface, and ICP-MS detection drift (see Pearce et al., 1997). The glass reference

244   material NIST SRM 612 was used as a calibration standard with the values of Pearce et al.

245   (1997). Precision (degree of reproducibility) and accuracy (degree of veracity) of the applied

246   method were controlled by repeated analyses of the glass reference material NIST SRM 614

247   (Li concentration value taken from Kurosawa et al., 2002). For each shell, the sequence of

248   analyses was as follows: $(NIST612)_{\times 2}$ + shell$_{\times 2}$ + (shell$_{\times 15}$ + NIST614 + shell$_{\times 15}$ +

249    $NIST612)_{\times 11}$ + NIST612. Data processing (including instrumental drift correction and

250   normalization) was performed using GLITTER v.4 software (Macquarie Research Ltd.,

251   Australia; Van Achterbergh et al., 2001), following the methods of Longerich et al. (1996).

252   Li/Ca detection limit at the 99% confidence level was calculated by GLITTER using

253   Poisson counting statistics and was 0.243 µmol mol^{-1}. Repeated measurements of NIST SRM

254   614 (n = 22) yielded a precision of 1.9 % (% RSD). Accuracy was extremely good with a Li

255   concentration value in NIST SRM 614 of 1.687 ± 0.007 µg g^{-1} compared with the

256   recommended value of 1.69 ± 0.026 µg g^{-1} (means ± standard errors).

257

258   **2.5. Statistical analyses**

259   Two different statistical tests were used to compare the means of two independent

260   samples: Student's *t*-test (large samples: min(n_1, n_2) ≥ 30) and Mann-Whitney *U*-test (small

261   samples: min(n_1, n_2) < 30). An analysis of covariance (ANCOVA; α = 0.05) was used to test

262   whether there were significant differences between the slopes of the least-square linear

263   regressions (Li/Ca$_{shell}$ vs. T$_{\delta 18O}$) calculated for each of the two shells. Homogeneity of residual

264   variances was tested with Bartlett's test (α = 0.01). No data were excluded. All statistical

265   analyses were performed according to Scherrer (1984).

266

267   **3. RESULTS**

268

269   **3.1. δ^{18}O$_{shell}$ profiles**

270   In each shell, δ^{18}O$_{shell}$ profile showed cyclical oscillations in phase with the main growth

271   lines that were revealed after the immersion of shell sections in Mutvei's solution (Fig. 3).

272   This confirms the annual periodicity of these growth lines. Seven main growth lines were

273   observed in both shells, suggesting that both specimens settled on the seafloor in 1999.

274   Isotopic data covered four full years of growth (2002-2005) and the beginning of year 2006.

275   δ^{18}O$_{shell}$ values ranged from 1.64 to 3.51 ‰ in shell A55 and from 1.73 to 3.45 ‰ in

276   shell A56. Annual minima ranged from 1.64 to 2.15 ‰, whereas annual maxima varied

13

277   between 2.92 and 3.51 ‰ (Table 2). Seasonal $\delta^{18}O_{shell}$ cycles were strongly right-skewed with

278   minimum/maximum values occurring shortly before/after the annual growth lines (Fig. 3).

279   These $\delta^{18}O_{shell}$ values were converted into temperature ($T_{\delta18O}$) using Eq. (1) and a

280     $\delta^{18}O_{water}$ value of -0.55 ‰ (Fig. 3). Annual minimum temperatures recorded by the shells

281   ranged from 1.8 to 4.4°C (mean [2002-2006] = 3.1°C; σ = 1.0°C; Table 2). Mean annual

282   minima in shells A55 (3.0°C) and A56 (3.3°C) were not significantly different from each

283   other (Mann-Whitney $U = 8.5$, $n_1 = n_2 = 5$, $p > 0.05$). Annual maximum temperatures

284   recorded by the shells ranged from 7.7 to 9.9°C (mean [2002-2005] = 8.5°C; σ = 0.8°C; Table

285   2). Mean annual maxima in shells A55 (8.4°C) and A56 (8.7°C) did not differ significantly

286   (Mann-Whitney $U = 5$, $n_1 = n_2 = 4$, $p > 0.05$).

287   The offsets between $T_{\delta18O}$ and T_{LA1} (0.3°C and 0.6°C for average annual minima and

288   maxima respectively) are within the ± 0.95°C uncertainty on $T_{\delta18O}$, so it is reasonable to

289   assume that the whole annual range of seawater temperature was recorded by the shells.

290

291   **3.2. Li/Ca$_{shell}$ profiles**

292   For both specimens, Li/Ca$_{shell}$ profiles showed cyclical variations with minimum values

293   recorded exactly at the annual growth lines (Fig. 3). A general tendency of the seasonal

294   Li/Ca$_{shell}$ variations was a progressive increase after the annual line, followed by a plateau and

295   then a decrease down to minimum values. Maximum Li/Ca$_{shell}$ values tended to occur earlier

296   during the growing season than $\delta^{18}O_{shell}$ minima (i.e. before temperature maxima; Fig. 3).

297   Li/Ca$_{shell}$ ranged from 7.00 to 9.40 µmol mol^{-1} in shell A55 (mean = 8.37 µmol mol^{-1};

298   Fig. 3a) and from 6.91 to 11.12 µmol mol^{-1} in shell A56 (mean = 9.23 µmol mol^{-1}; Fig. 3b).

299   Mean Li/Ca$_{shell}$ ratio was significantly higher in shell A56 than in shell A55 (t-test $t = 16.87$,

300     $n_1 = n_2 = 332$, $p < 0.01$).

14

301   Annual minimum values ranged from 7.00 to 7.29 µmol mol^{-1} in shell A55 (mean

302   [2001-2005] = 7.16 µmol mol^{-1}; σ = 0.12 µmol mol^{-1}), and from 7.10 to 7.64 µmol mol^{-1} in

303   shell A56 (mean [2002-2005] = 7.44 µmol mol^{-1}; σ = 0.23 µmol mol^{-1}; Table 3). Mean annual

304   minima in shells A55 and A56 did not differ significantly (Mann-Whitney $U = 3$, $n_1 = 5$, $n_2 =$

305   4, $p > 0.05$).

306   Annual maxima ranged from 9.08 to 9.40 µmol mol^{-1} in shell A55 (mean [2001-2005] =

307   9.30 µmol mol^{-1}; σ = 0.13 µmol mol^{-1}), and from 10.03 to 11.12 µmol mol^{-1} in shell A56

308   (mean [2002-2005] = 10.46 µmol mol^{-1}; σ = 0.22 µmol mol^{-1}; Table 3). Mean annual

309   maximum in shell A56 was significantly higher than in shell A55 (Mann-Whitney $U = 0$, $n_1 =$

310   5, $n_2 = 4$, $p < 0.05$).

311   As a consequence, mean annual amplitude in shells A55 (2.14 µmol mol^{-1}) and A56

312   (3.02 µmol mol^{-1}) were significantly different (Mann-Whitney $U = 0$, $n_1 = 5$, $n_2 = 4$, $p < 0.05$).

313   Annual amplitude ranged from 2.01 to 2.32 µmol mol^{-1} in shell A55, and from 2.76 to 3.63

314   µmol mol^{-1} in shell A56 (Table 3).

315   Li/Ca$_{shell}$ in both shells was statistically correlated with the δ^{18}O$_{shell}$-derived temperature

316   ($p < 0.05$ for both specimens; Fig. 4). An ANCOVA showed no significant difference

317   between slopes of the two linear regressions (Bartlett's test: $B_C = 5.52$, $df = 1$; ANCOVA: $F =$

318   0.02, $df = 1$ and 95). The strength of these correlations was, however, extremely weak with

319   determination coefficients ranging from 0.11 (shell A56) to 0.25 (shell A55). The difference

320   in intercept values (ca. 1 µmol mol^{-1}) reflects the difference in annual maxima between shell

321   A56 and shell A55.

322   The comparison of Li/Ca$_{shell}$ variations with daily shell growth rates was difficult

323   because we were unexpectedly unable to resolve microgrowth structures over the whole shell

324   sections despite etching with Mutvei's solution. Nevertheless, 22 groups of 3-5 microgrowth

325   increments were quite clearly revealed in the A56 shell portion formed in 2004. The average

326   increment width in each of these 22 batches was calculated and plotted with the A56 Li/Ca_{shell}

327   record for year 2004 (Fig. 5a). Although the number of increment data was limited, our data

328   showed that Li/Ca_{shell} covaried with microgrowth increment width, which ranged from 24-28

329   µm near the annual lines to 43 µm in the first half of the 2004 growing season (average = 32.3

330   µm). A simple linear regression indicated that microgrowth increment width explained 53%

331   of the Li/Ca_{shell} variability in shell A56 ($p < 0.001$; Fig. 5b). Note that all geochemical and

332   shell growth data obtained on specimens A55 and A56 can be retrieved in the auxiliary

333   material.

334

335   **4. DISCUSSION**

336

337   **4.1. Seasonal timing of geochemical records in shells**

338   The present study is the first to investigate Li/Ca records in bivalve shells. Li/Ca_{shell}

339   seasonal variations in our two *Arctica islandica* specimens were well-marked, presenting a

340   1.3- to 1.6-fold range over a given growing season (Fig. 3). The inter-annual variability

341   between ontogenetic ages 3 to 8 was far less pronounced than intra-annual variability.

342   Combined analyses of Li/Ca_{shell} and $\delta^{18}O_{shell}$, and reconstruction of seawater temperature from

343    $\delta^{18}O_{shell}$ allowed us to estimate the seasonal timing of Li/Ca_{shell} variations.

344        $T_{\delta18O}$ variations (average annual range = 3.1 – 8.5°C) showed that the whole annual

345   range of seawater temperature (2.8 to 7.9°C at 20 m depth at LA1) was recorded by the shells

346   (Table 2). This implies that *A. islandica* shells did not stop growing because of thermal stress.

347   Conversely, the position of the annual growth breaks between minimum and maximum

348    $\delta^{18}O_{shell}$ (i.e. between maximum and minimum temperatures, recorded in August and March,

349   respectively) suggests that shells stopped growing between September and February. The

350   average microgrowth increment width measured in shell A56 was 32.3 µm at ontogenetic age

351   6, i.e. similar to the value calculated by Schöne et al. (2005a) for North Sea specimens (31.5

352   μm at ontogenetic age 4). This suggests that shell growth lasted ca. 185 days to achieve the

353   5.96 mm width of the 2004 annual increment. This result supports the hypothesis of a ca. 6-

354   month growth break between September and February. As minimum temperatures were

355   recorded by $\delta^{18}O_{shell}$, shells did not stop growing because of harsh winter conditions. Schöne

356   et al. (2005a) showed that *A. islandica* specimens from the North Sea stopped growing from

357   early September to mid-November and described this growth break as a spawning biocheck.

358   In Iceland, *A. islandica* spawning activity peaks in June-July, whereas gametogenesis occurs

359   from January to May (Thorarinsdóttir, 2000). Therefore, the annual growth breaks found in

360   our specimens cannot be attributed to reproductive activity. Moreover, our specimens were

361   likely juveniles as in Icelandic waters, only 10% of *A. islandica* of 40 mm shell length are

362   mature (Thorarinsdóttir and Jacobson, 2005). Therefore, the origin of these annual growth

363   breaks remains unclear. Their investigation, however, is far beyond the goals of this paper.

364   The most important point is that the timing of the growing season determined by $T_{\delta18O}$

365   variations allowed us to conclude that Li/Ca_{shell} increases from March to May, i.e. right after

366   the annual line, stays roughly stable in June, and then decreases in July–August.

367

4.2. Processes potentially involved in Li/Ca$_{shell}$ seasonal variations

369   The shape of Li/Ca_{shell} variations is very similar in shells A55 and A56 and as such this

370   ratio likely responds to environmental variations or to variations of a physiological process

371   synchronized within a given population by genetic and/or exogenous factors. Based on

372   published literature on Li/Ca ratios in $CaCO_3$ structures, the following parameters may

373   provide plausible hypotheses to explain the Li/Ca_{shell} variations in *A. islandica*: temperature,

374   calcification rate, and Li/Ca ratio in seawater. Their potential influence on the shell

375   geochemistry will be discussed in light of the evidence presented here. A fourth hypothesis

376   will also be put forward: the influence of suspended Li-rich particles originating from the

377   mechanical weathering of basaltic rocks.

378

379   *4.2.1. Temperature*

380   Several studies have found a significant inverse relationship between Li/Ca in $CaCO_3$

381   structures and temperature in coralline aragonite (Marriott et al., 2004b; Montagna et al.,

382   2006), in foraminiferal calcite (Hall and Chan, 2004; Marriott et al., 2004a), in calcitic

383   brachiopods (Delaney et al., 1989), and in inorganic calcite (Marriott et al., 2004b). We also

384   found relationships with temperature in *A. islandica* aragonitic shells but these were positive,

385   not negative (Fig. 4). Unlike these previous studies, our findings agree with thermodynamic

386   calculations predicting that Li concentration in $CaCO_3$ structures should decrease with

387   decreasing temperature (Hall and Chan, 2004). According to Okumura and Kitano (1986), Li

388   is incorporated in the crystal structure of aragonite in substitution of Ca, leading to the

389   formation of lithium carbonate (Li_2CO_3) crystals. Smith et al. (1971) showed that the

390   solubility of Li_2CO_3 increases with decreasing temperature. In other words, crystallization of

391   Li_2CO_3 becomes easier as temperature rises (an almost linear relationship between 0 and

392   30°C; Smith et al., 1971). Although statistically significant ($p < 0.05$), the strength of our

393   temperature-Li/Ca_{shell} relationships is extremely weak ($0.11 < r^2 < 0.25$). The weakness of this

394   relationship is particularly obvious for the 2003 Li/Ca_{shell} record in shell A56 where an

395   important offset can be seen between Li/Ca_{shell} and $\delta^{18}O_{shell}$ (Fig. 3b). Our findings suggest

396   that if temperature-dependant solubility of Li_2CO_3 really plays a role on Li/Ca_{shell} in

397   *A. islandica*, this influence is extremely weak.

398

399   *4.2.2. Calcification rate*

18

400   Many authors have suggested that the main factor controlling Li incorporation in

401   foraminiferal calcite could be calcification rate, which may itself correlate partly with

402   temperature (Delaney et al., 1985; Hall and Chan, 2004; Marriott et al, 2004a). According to

403   Carré et al. (2006), crystal growth rate strongly influences incorporation of Sr, Ba, Mn, and

404   Mg in aragonitic shells of two Peruvian bivalve species (*Mesodesma donacium* and *Chione*

405   *subrugosa*). However, they did not investigate Li/Ca$_{shell}$ ratios. Our own results seem to

406   support these findings. Indeed, we found a relatively strong relationship between microgrowth

407   increment width and Li/Ca in *A. islandica* shells (Fig. 5). Although microgrowth increment

408   width represents the dorso-ventral linear extension of the shell per unit time and may slightly

409   differ from the absolute calcification rate (see Gillikin et al. (2005) for elaboration), our

410   results suggest that Li/Ca$_{shell}$ may increase as a direct response of increasing calcification rate.

411   Another argument in favor of this hypothesis is the difference observed in the range of Li/Ca

412   variations in shells A55 and A56; although these two specimens appeared to have grown at an

413   equivalent annual rate from 1999 to 2006, it can be assumed that A56 reached higher daily

414   growth rates in summer than A55, explaining the difference in annual Li/Ca$_{shell}$ maxima

415   between these two shells. The mechanisms involved in these vital effects are unknown and

416   any discussion on that subject would be highly speculative due to the scarcity of studies

417   dealing with the formation of Li_2CO_3 crystals within aragonitic structures. Identification of

418   these mechanisms would require biomineralization and/or inorganic precipitation

419   experiments.

420

421   *4.2.3. Li/Ca$_{seawater}$*

422   Delaney et al. (1985) and Hathorne and James (2006) suggested that Li/Ca ratio in

423   calcitic foraminifera was directly controlled by the Li/Ca of the growing medium. Could

424   possible variations of Li/Ca$_{seawater}$ over *A. islandica* growing season have an influence on the

425   shell geochemistry? Li is essentially conservative in seawater with an almost constant

426   concentration of 26 µmol L^{-1} and a Li/Ca$_{seawater}$ ratio of ca. 2310 µmol mol^{-1} (Li, 2000). It has

427   no significant involvement in biological activity or scavenging by particles (Stoffyn-Egli and

428   Mackenzie, 1984). Given the long residence times of Li (1.5 million years; Huh et al., 1998)

429   and Ca (1 million year; Broecker and Peng, 1982), the Li/Ca ratio of the global ocean has

430   probably not changed over the Holocene (Hall and Chan, 2004). The two major sources of Li

431   to the ocean are (1) high-temperature basalt-seawater reactions, and (2) river input from the

432   weathering of continental crust (Hoefs and Sywall, 1997). In hydrothermal systems near the

433   mid-ocean ridges, Li is leached from oceanic basalts at temperatures >250°C (Hoefs and

434   Sywall, 1997). Although the mid-Atlantic ridge runs right through Iceland, it is unlikely that

435   such high temperatures could be reached at shallow coastal locations. Moreover, it is hardly

436   conceivable that Li leaching from this ridge would follow a seasonal pattern; it is rather

437   roughly constant throughout the year. Therefore, high-temperature hydrothermal circulation

438   can certainly not explain Li/Ca$_{shell}$ seasonal variations.

439   Seasonal variations of riverine inputs may, however, have a local influence on Li/Ca

440   ratios in coastal waters. Intensities of chemical and mechanical weathering of silicate rocks

441   like basalts are usually expressed in terms of fluxes of dissolved and suspended materials,

442   respectively (Gislason et al., 2009). Gislason et al. (2009) found a relationship between air

443   temperature and chemical weathering rate in 8 northeastern Iceland river catchments. Air

444   temperature in Iceland starts increasing in March and reaches maxima in July. Intensity of

445   chemical weathering may therefore follow the same general pattern as Li/Ca$_{shell}$. Pogge von

446   Strandmann et al. (2006) analyzed the chemical composition of 25 Icelandic rivers in

447   September 2003 and August 2005 and found an average dissolved Li concentration of 87.5

448   nmol L^{-1} (range: 1.54–1250 nmol L^{-1}) and a Li/Ca$_{river}$ ratio ranging from 31 to 2461 µmol

449   mol^{-1} (average = 563 µmol mol^{-1}). This dissolved Li concentration range is similar to that

450   measured by Vigier et al. (2009) in the major Icelandic rivers (range: 3–317 nmol L^{-1}; average

451   = 86.5 nmol L^{-1}). These values may be slightly higher in July, ie. at the annual air temperature

452   maximum. According to Delaney et al. (1985), a 1.8 to 2.6-fold increase of the average

453   Li/Ca$_{seawater}$ ratio is necessary to observe a 1.3 to 1.6-fold increase of Li/Ca in calcitic

454   foraminifera. This relationship can probably not be applied to *A. islandica* shells because of

455   their aragonitic structure. Nevertheless, it highlights that Li/Ca$_{seawater}$ must increase

456   significantly to induce a 1.3 to 1.6-fold increase of Li/Ca in biogenic carbonates. Given that

457   the maximum Li/Ca$_{river}$ ratio measured by Pogge von Strandmann et al. (2006) was only 1.1-

458   fold higher than Li/Ca$_{seawater}$, seasonal variations of basalt chemical weathering and dissolved

459   Li flux can hardly explain the full variability of Li/Ca$_{shell}$ in *A. islandica*.

460

461   *4.2.4. Suspended Li-rich basaltic particles*

462   A fourth hypothesis could be put forward to explain Li/Ca$_{shell}$ seasonal variations: the

463   possible influence of weathered basaltic particles carried by rivers. Seasonal variations of

464   Sandá River discharge were obtained from the Hydrological Service of the Icelandic National

465   Energy Authority (http://www.os.is/; Fig. 6). These data show that discharge roughly follows

466   the same seasonal pattern as Li/Ca$_{shell}$, with values ranging from ca. 10 m^3 s^{-1} in fall and

467   winter to ca. 35 m^3 s^{-1} in June (long term average). Could these variations in river discharge

468   induce large changes in the flux of suspended particles? Gislason et al. (2009) described and

469   quantified a direct relationship between river discharge and mechanical weathering (expressed

470   as suspended inorganic material (SIM) flux) in 8 river catchments in northeast Iceland.

471   Depending on which of their 8 discharge-SIM flux equations is used for calculation, the 350%

472   seasonal increase in river discharge would induce a 350 to 4900% increase in SIM flux over a

473   year. Therefore, high loads of suspended basaltic particles probably flow to the sea with

474   Icelandic rivers as soon as the snow melts, reaching a peak roughly at the same time as the

475   Li/Ca$_{shell}$ annual maximum. These river particles have a high Li content (several ppm; Pogge

476   von Strandmann et al., 2006), ca. 1 order of magnitude larger than in shells. Although the

477   freshwater inputs likely flow as a thin surface layer (ca. 10 meters thickness; cf. Assthorsson,

478   1990; Andrews et al., 2001), it is likely that suspended material carried by rivers can cross the

479   halocline and settle on the seafloor, thus modifying the chemistry of bottom waters.

480   Consequently, these Li-rich particles may significantly increase Li/Ca$_{shell}$, either directly (if

481   ingested, transferred to the internal fluids, and then incorporated within the shell during

482   biomineralization) or indirectly if they weather after deposition on the seafloor. This

483   hypothesis could be tested in further studies through analyses of the lithium isotope

484   composition of *A. islandica* shells. SIM originating from the weathering of basaltic material

485   has a very low δ^7Li value (δ^7Li_{SIM} = $-$ 1.3 to 7.5‰ in Icelandic rivers; Pogge von Strandmann

486   et al., 2006) in comparison to seawater ($\delta^7Li_{seawater}$ = 32‰; Huh et al., 1998). If indeed Li

487   incorporation in shells is linked to Li-rich particle inputs by rivers, then shell aragonite must

488   have a δ^7Li several per mil lighter than seawater.

489

490   **4.3. Conclusions**

491   Lithium is likely incorporated in *A. islandica* aragonitic shells as lithium carbonate

492   Li$_2$CO$_3$, i.e. Li$^+$ substitutes for Ca^{2+} at the site of calcification in the extrapallial fluid. Several

493   explanations could account for the observed seasonal variations in Li/Ca ratio in shells:

494   1 - The significant positive relationship found between $\delta^{18}O_{shell}$-derived temperature and

495   Li/Ca$_{shell}$ suggests that seasonal Li/Ca$_{shell}$ variations could be linked to increasing solubility of

496   Li$_2$CO$_3$ with decreasing temperature in the extrapallial fluid. However, the strength of this

497   relationship is so weak that temperature-dependant solubility of Li$_2$CO$_3$ cannot possibly be

498   the main factor controlling Li/Ca$_{shell}$ variations;

499   2 - Given the strong and significant positive relationship found between Li/Ca$_{shell}$ and

500   microgrowth increment width, Li/Ca$_{shell}$ may partly be controlled by variations in calcification

501   rate. As this rate is also partly controlled by temperature, it is difficult to make conclusions

502   about the exact importance of Li$_2$CO$_3$ solubility in Li/Ca$_{shell}$ variations;

503   3 - Sandá river discharge and Li/Ca$_{shell}$ presented an intriguing similarity in their seasonal

504   variations. As soon as snow melts in spring, mechanical weathering of basaltic rocks gains

505   intensity due to the increased river discharge, leading to a massive flow of Li-rich silicate

506   particles into the ocean. This phenomenon reaches a peak at the same time as Li/Ca$_{shell}$. We

507   therefore suggest that this massive input of Li could be trapped in the shell, thus impacting

508   Li/Ca$_{shell}$.

509   If indeed Li/Ca$_{shell}$ is mainly controlled by calcification rate, then this ratio may be

510   useful to address seasonal variations in growth rate of bivalve species in which daily growth

511   increments and lines are not easily discernable. In turn, abrupt decreases of Li/Ca$_{shell}$ may be

512   helpful to identify growth retardations, for instance related to the occurrence of toxic

513   phytoplankton blooms in coastal ecosystems. Alternatively, if Li/Ca$_{shell}$ in *A. islandica* is

514   controlled by river inputs of Li-rich silicate particles, it may then be used a proxy for the

515   intensity of mechanical weathering of Icelandic basaltic rocks. This could have exciting

516   perspectives, e.g. to get a better insight about the frequency and intensity of past jökulhlaups

517   (subglacial outburst floods). It may also be interesting to analyze the geochemical

518   composition of recent *A. islandica* shells from the south-east coast of Iceland, where a huge

519   jökulhlaup flowed under the Vatnajökull glacier in 1996 because of the subglacial eruption of

520   the Grímsvötn Volcano. In any event, it is clear from our work that further studies, including

521   δ^7Li$_{shell}$ analyses and experiments under controlled conditions, are needed to better understand

522   Li/Ca$_{shell}$ variations in bivalve shells and to determine if this could be a useful proxy for

523   paleoecological reconstructions.

524   **ACKNOWLEDGMENTS**

525

543   **REFERENCES**

544

545   Andrews, J. T., C. Caseldine, N. J. Weiner, and J. Hatton (2001), Late Holocene (ca. 4 ka)

546   marine and terrestrial environmental change in Reykjarfjördur, north Iceland: climate

547   and/or settlement?, *J. Quarter. Sci.*, *16*, 133-143.

548   Astthorsson, O. S. (1990), Ecology of the euphausiids *Thysanoessa raschi*, *T. inermi*s and

549   *Meganyctiphanes norvegica* in Ísafjord-deep, northwest-Iceland, *Mar. Biol.*, *107*, 147-

550   157.

551   Broecker, W. S., and T.-H. Peng (Eds.) (1982), *Tracers in the sea*, 690 pp., Eldigio Press,

552   Palisades.

553   Carré, M., I. Bentaleb, O. Bruguier, E. Ordinola, N. T. Barrett, and M. Fontugne (2006),

554   Calcification rate influence on trace element concentrations in aragonitic bivalve shells:

555   Evidences and mechanisms, *Geochim. Cosmochim. Acta*, *70*, 4906-4920.

556   Carriker, M. R., C. P. Swann, J. Ewart, and C. L. Counts III (1996), Ontogenetic trends of

557   elements (Na to Sr) in prismatic shell of living *Crassostrea virginica* (Gmelin) grown in

558   three ecologically dissimilar habitats for 28 weeks: a proton probe study, *J. Exp. Mar.*

559   *Biol. Ecol.*, *201*, 87-135.

560   Chauvaud, L., A. Lorrain, R. B. Dunbar, Y.-M. Paulet, G. Thouzeau, F. Jean, J.-M. Guarini,

561   and D. Mucciarone (2005), Shell of the Great Scallop *Pecten maximus* as a high-

562   frequency archive of paleoenvironmental changes, *Geochem. Geophys. Geosystems*,

563   *6*(8), Q08001, doi:10.1029/2004GC000890.

564   Craig, C.-A., K. E. Jarvis, and L. J. Clarke (2000), An assessment of calibration strategies for

565   the quantitative and semi-quantitative analysis of calcium carbonate matrices by laser

566   ablation-inductively coupled plasma-mass spectrometry (LA-ICP-MS), *J. Anal. At.*

567   *Spectrom.*, *15*, 1001-1008.

568   Delaney, M. L., A. W. H. Bé, and E. A. Boyle (1985), Li, Sr, Mg, and Na in foraminiferal
569   calcite shells from laboratory culture, sediment traps, and sediment cores, *Geochim.*
570   *Cosmochim. Acta*, *49*, 1327-1341.

571   Delaney, M. L., B. N. Popp, C. G. Lepzelter, and T. F. Anderson (1989), Lithium-to-calcium
572   ratios in modern, Cenozoic, and Paleozoic articulate brachiopod shells,
573   *Paleoceanography*, *4*, 681-691.

574   Dick, D., E. Philipp, M. Kriews, and D. Abele (2007), Is the umbo matrix of bivalve shells
575   (*Laternula elliptica*) a climate archive?, *Aquat. Toxicol.*, 84, 450-456.

576   Epplé, V. M. (2004), High-resolution climate reconstruction for the Holocene based on
577   growth chronologies of the bivalve *Arctica islandica* from the North Sea, Ph.D. thesis,
578   101 pp., University of Bremen, 17 December.

579   Epstein, S., R. Buchsbaum, H. A. Lowenstam, and H. C. Urey (1953), Revised carbonate-
580   water isotopic temperature scale, *Bull. Geol. Soc. Am.*, *64*, 1315-1326.

581   Fiebig, J., B. R. Schöne, and W. Oschmann (2005), High-precision oxygen and carbon
582   isotope analysis of very small (10–30 μg) amounts of carbonates using continuous flow
583   isotope ratio mass spectrometry, *Rapid Commun. Mass Spectrom.*, *19*, 2355-2358.

584   Gillikin, D. P., A. Lorrain, J. Navez, J. W. Taylor, L. André, E. Keppens, W. Baeyens, and F.
585   Dehairs (2005), Strong biological controls on Sr/Ca ratios in aragonitic marine bivalve
586   shells, *Geochem. Geophys. Geosystems*, *6*(5), Q05009, doi:10.1029/2004GC000874.

587   Gislason, S. R., et al. (2009), Direct evidence of the feedback between climate and
588   weathering, *Earth and Planetary Science Letters*, *277*, 213-222.

589   Grossman, E. L., and T.-L. Ku (1986), Oxygen and carbon isotope fractionation in biogenic
590   aragonite; temperature effects, *Chem. Geol.*, *59*, 59-74.

591   Hall, J. M., and L.-H. Chan (2004), Li/Ca in multiple species of benthic and planktonic

592   foraminifera: thermocline, latitudinal, and glacial-interglacial variation, *Geochim.*

593   *Cosmochim. Acta*, *68*, 529-545.

594   Hathorne, E. C., and R. H. James (2006), Temporal record of lithium in seawater: A tracer for

595   silicate weathering?, *Earth Planet. Sci. Lett.*, *246*, 393-406.

596   Henderson, G. M. (2002), New oceanic proxies for paleoclimate, *Earth Planet. Sci. Lett.*, *203*,

597   1-13.

598   Hoefs, J., and M. Sywall (1997), Lithium isotope composition of quaternary and tertiary

599   biogene carbonates and a global lithium isotope balance, *Geochim. Cosmochim. Acta*,

600   *61*, 2679-2690.

601   Hopkins, T. S. (1991), The GIN Sea - a synthesis of its physical oceanography and literature

602   review 1972-1985, *Earth Sci. Rev.*, *30*, 175-318.

603   Huh, Y., L.-H. Chan, L. Zhang, and J. M. Edmond (1998), Lithium and its isotopes in major

604   world rivers: implications for weathering and the oceanic budget, *Geochim. Cosmochim.*

605   *Acta*, *62*, 2039-2051.

606   Hut, G. (1987), Consultants' group meeting on stable isotope reference samples for

607   geochemical and hydrological investigations, *Report to the Director General*, 44 pp.,

608   International Atomic Energy Agency, Vienna.

609   Jones, D. S. (1983), Sclerochronology: Reading the record of the molluscan shell, *Am. Sci.*,

610   *71*, 384-391.

611   Jones, D. S. (1998), Isotopic determination of growth and longevity on fossil and modern

612   invertebrates, *Palaeontol. Soc. Pap.*, *4*, 37-67.

613   Kilada, R. W., S. E. Campana, and D. Roddick (2007), Validated age, growth, and mortality

614   estimates of the ocean quahog (*Arctica islandica*) in the western Atlantic, *ICES J. Mar.*

615   *Sci.*, *64*, 31-38.

616   Kurosawa, M., S. E. Jackson, and S. Sueno (2002), Trace element analysis of NIST SRM 614

617   and 616 glass reference materials by Laser Ablation Microprobe-Inductively Coupled

618   Plasma-Mass Spectrometry, *Geostand. Geoanal. Res.*, *26*, 75-84.

619   Li, Y.-H. (Ed.) (2000), *A compendium of geochemistry: From solar nebula to the human*

620   *brain*, 440 pp., Princeton University Press, Princeton.

621   Liehr, G. A., M. L. Zettler, T. Leipe, and G. Witt (2005), The ocean quahog *Arctica islandica*

622   L.: a bioindicator for contaminated sediments, *Mar. Biol.*, *147*, 671-679.

623   Lindh, U., H. Mutvei, T. Sunde, and T. Westermark (1988), Environmental history told by

624   mussel shells, *Nucl. Instr. Meth. Phys. Res. B*, *30*, 388-392.

625   Lingard, S. M., R. D. Evans, and B. P. Bourgoin (1992), Method for the estimation of

626   organic-bound and crystal-bound metal concentrations in bivalve shells, *Bull. Environ.*

627   *Contam. Toxicol.*, *48*, 179-184.

628   Longerich, H. P., S. E. Jackson, and D. Günther (1996), Laser ablation inductively coupled

629   plasma mass spectrometric transient signal data acquisition and analyte concentration

630   calculation, *J. Anal. At. Spectrom.*, *11*, 899-904.

631   Marchitto, T. M., G. A. Jones, G. A. Goodfriend, and C. R. Weidman (2000), Precise

632   temporal correlation of Holocene mollusk shells using sclérochronologie, *Quat. Res.*,

633   *53*, 236-246.

634   Marin, F., and G. Luquet (2004), Molluscan shell proteins, *C. R. Palevol*, *3*, 469-492.

635   Marriott, C. S., G. M. Henderson, R. Crompton, M. Staubwasser, and S. Shaw (2004a), Effect

636   of mineralogy, salinity, and temperature on Li/Ca and Li isotope composition of calcium

637   carbonate, *Chem. Geol.*, *212*, 5-15.

638   Marriott, C. S., G. M. Henderson, N. S. Belshaw, and A. W. Tudhope (2004b), Temperature

639   dependence of δ^7Li, δ^{44}Ca and Li/Ca during growth of calcium carbonate, *Earth Planet.*

640   *Sci. Lett.*, *222*, 615-624.

641 McCrea, J. M. (1950), On the isotopic chemistry of carbonates and a paleotemperature scale,

642   *J. Chem. Phys.*, *18*, 849-857.

643 Montagna, P., M. McCulloch, C. Mazzoli, S. Silenzi, and S. Schiaparelli (2006), Li/Ca ratios

644   in the Mediterranean non-tropical coral *Cladocora caespitosa* as a potential

645   paleothermometer, *Geophys. Res. Abstr.*, *8*, Abstract 03695.

646 Okumura, M., and Y. Kitano (1986), Coprecipitation of alkali metal ions with calcium

647   carbonate, *Geochim. Cosmochim. Acta*, *50*, 49-58.

648 Pannella, G., and C. McClintock (1968), Biological and environmental rhythms reflected in

649   molluscan shell growth, *J. Paleontol.*, *42*, 64-80.

650 Pearce, N. J. G., W. T. Perkins, J. A. Westgate, M. P. Gorton, S. E. Jackson, C. R. Neal, and

651   S. P. Chenery (1997), A compilation of new and published major and trace element data

652   for NIST SRM 610 and NIST SRM 612 glass reference materials, *Geostand. Geoanal.*

653   *Res.*, *21*, 115-144.

654 Pogge von Strandmann, P. A. E., K. W. Burton, R. H. James, P. van Calsteren, S. R. Gíslason,

655   and F. Mokadem (2006), Riverine behaviour of uranium and lithium isotopes in an

656   actively glaciated basaltic terrain, *Earth Planet. Sci. Lett.*, *251*, 134-147.

657 Scherrer, B. (1984), *Biostatistiques*, 850 pp., Gaëtan Morin Editeur, Québec.

658 Schmidt, G.A., G. R. Bigg, and E. J. Rohling (1999), Global seawater oxygen-18 database,

659   http://data.giss.nasa.gov/o18data/, Goddard Institute for Space Studies, New York.

660 Schöne, B. R. (2008), The curse of physiology—challenges and opportunities in the

661   interpretation of geochemical data from mollusk shells, *Geo-Marine Lett.*, *28*, 269-285.

662 Schöne, B. R., W. Oschmann, J. Rössler, A. D. Freyre Castro, S. D. Houk, I. Kröncke, W.

663   Dreyer, R. Janssen, H. Rumohr, and E. Dunca (2003), North Atlantic Oscillation

664   dynamics recorded in shells of a long-lived bivalve mollusk, *Geology*, *31*, 1037-1040.

665   Schöne, B. R., A. D. Freyre Castro, J. Fiebig, S. D. Houk, W. Oschmann, and I. Kröncke

666   (2004), Sea surface water temperatures over the period 1884–1983 reconstructed from

667   oxygen isotope ratios of a bivalve mollusk shell (*Arctica islandica*, southern North Sea),

668   *Palaeogeogr. Palaeoclimatol. Palaeoecol.*, *212*, 215-232.

669   Schöne, B. R., S. D. Houk, A. D. Freyre Castro, J. Fiebig, W. Oschmann, I. Kröncke, W.

670   Dreyer, and F. Gosselck (2005a), Daily growth rates in shells of *Arctica islandica*:

671   Assessing sub-seasonal environmental controls on a long-lived bivalve mollusk,

672   *Palaios*, *20*, 78-92.

673   Schöne, B. R., J. Fiebig, M. Pfeiffer, R. Gleß, J. Hickson, A. L. A. Johnson, W. Dreyer, and

674   W. Oschmann (2005b), Climate records from a bivalved Methuselah (*Arctica islandica*,

675   Mollusca; Iceland), *Palaeogeogr. Palaeoclimatol. Palaeoecol.*, *228*, 130-148.

676   Schöne, B. R., M. Pfeiffer, T. Pohlmann, and F. Siegismund (2005c), A seasonally resolved

677   bottom-water temperature record for the period AD 1866-2002 based on shells of

678   *Arctica islandica* (Mollusca, North Sea), *Int. J. Climatol., 25*, 947-962.

679   Schöne, B. R., E. Dunca, J. Fiebig, and M. Pfeiffer (2005d), Mutvei's solution: An ideal agent

680   for resolving microgrowth structures of biogenic carbonates, *Palaeogeogr.*

681   *Palaeoclimatol. Palaeoecol.*, *228*, 149-166.

682   Smith, S. H., D. D. Williams, and R. R. Miller (1971), Solubility of lithium carbonate at

683   elevated temperatures, *J. Chem. Eng. Data*, *16*, 74-75.

684   Stecher III, H. A., D. E. Krantz, C. J. Lord III, G. W. Luther III, and K. W. Bock (1996),

685   Profiles of strontium and barium in *Mercenaria mercenaria* and *Spisula solidissima*

686   shells, *Geochim. Cosmochim. Acta*, *60*, 3445-3456.

687   Stoffyn-Egli, P., and F. T. Mackenzie (1984), Mass balance of dissolved lithium in the

688   oceans, *Geochim. Cosmochim. Acta*, *48*, 859-872.

689 Thébault, J., L. Chauvaud, J. Clavier, J. Guarini, R. B. Dunbar, R. Fichez, D. A. Mucciarone,

690   and E. Morize (2007), Reconstruction of seasonal temperature variability in the tropical

691   Pacific Ocean from the shell of the scallop, *Comptopallium radula. Geochim.*

692   *Cosmochim. Acta*, *71*, 918-928.

693 Thébault, J., L. Chauvaud, S. L'Helguen, J. Clavier, A. Barats, S. Jacquet, C. Pécheyran, and

694   D. Amouroux (2009), Barium and molybdenum records in bivalve shells: geochemical

695   proxies for phytoplankton dynamics in coastal environments?, *Limnol. Oceanogr.*, *54*,

696   1002-1014.

697 Thorarinsdóttir, G. G. (2000), Annual gametogenic cycle in ocean quahog, *Arctica islandica*

698   from north-western Iceland, *J. Mar. Biol. Assoc. U. K.*, *80*, 661-666.

699 Thorarinsdóttir, G. G., and L. D. Jacobson (2005), Fishery biology and biological reference

700   points for management of ocean quahogs (*Arctica islandica*) off Iceland, *Fish. Res.*, *75*,

701   97-106.

702 Toland, H., B. Perkins, N. Pearce, F. Keenan, and M. J. Leng (2000), A study of

703   sclerochronology by laser ablation ICP-MS, *J. Anal. At. Spectrom.*, *15*, 1143-1148.

704 Van Achterbergh, E., C. G. Ryan, S. E. Jackson, and W. L. Griffin (2001), Data reduction

705   software for LA-ICP-MS, in *Laser ablation-ICPMS in the earth sciences: principles*

706   *and applications*, edited by P. J. Sylvester, pp. 239-243, Mineralogical Association of

707   Canada Short Course Series 29, Ottawa.

708 Vander Putten, E., F. Dehairs, E. Keppens, and W. Baeyens (2000), High resolution

709   distribution of trace elements in the calcite shell layer of modern *Mytilus edulis*:

710   environmental and biological controls, *Geochim. Cosmochim. Acta*, *64*, 997-1011.

711 Vigier, N., S. R. Gislason, K. W. Burton, R. Millot, and F. Mokadem (2009), The relationship

712   between riverine lithium isotope composition and silicate weathering rates in Iceland,

713   *Earth Planet. Sci. Lett.*, doi: 10.1016/j.epsl.2009.08.026.

714   Wanamaker, A. D., J. Heinemeier, J. D. Scourse, C. A. Richardson, P. G. Butler, J. Eiríksson,

715   and K. L. Knudsen (2008a), Very-long lived molluscs confirm 17th century AD tephra-

716   based radiocarbon reservoir ages for north Icelandic shelf waters, *Radiocarbon*, *50*, 399-

717   412.

718   Wanamaker, A. D., K. J. Kreutz, B. R. Schöne, N. Pettigrew, H. W. Borns, D. S. Introne, D.

719   Belknap, K. A. Maasch, and S. Feindel (2008b), Coupled North Atlantic slope water

720   forcing on Gulf of Maine temperatures over the past millennium, *Clim. Dyn.*, *31*, 183-

721   194.

722   Wefer, G., W. H. Berger, J. Bijma, and G. Fischer (1999), Clues to ocean history: a brief

723   overview of proxies, in *Use of proxies in paleoceanography: examples from the South

724   Atlantic*, edited by G. Fischer and G. Wefer, pp. 1-68, Springer-Verlag, Berlin.

725   Weidman, C. R., G. A. Jones, and K. C. Lohmann (1994), The long-lived mollusc *Arctica

726   islandica*: A new paleoceanographic tool for the reconstruction of bottom temperatures

727   for the continental shelves of the northern North Atlantic Ocean, *J. Geophys. Res.*, *99*,

728   18305-18314.

729   Witbaard, R. (1997), Tree of the sea: The use of the internal growth lines in the shell of

730   *Arctica islandica* (Bivalvia, Mollusca) for the retrospective assessment of marine

731   environmental change, Ph.D. thesis, 157 pp., Rijksuniversiteit Groningen, 30 May.

732

733   **TABLES**

734

735   Table 1. LA-ICP-MS operating conditions.

736

Laser: New Wave Research UP-213		ICP-MS: Agilent 7500ce	
Crystal	Nd:YAG	RF power	1200 W
Wavelength	213 nm	Plasma gas flow	15 L min^{-1}
Laser mode	Q-switched	Auxiliary gas flow	1 L min^{-1}
Laser power	0.2 mJ	Carrier gas flow	0.65 L min^{-1}
Repetition rate	10 Hz	Optional gas flow	75% He
Pit diameter	80 µm	Acquisition mode	Pulse counting
Ablation time	60 s	Acquisition time	120 s
Background	60 s	Dwell time	10 ms

737

738   Table 2. Annual amplitudes of $\delta^{18}O_{shell}$ and $T_{\delta18O}$ of specimens A55 and A56 over the period

739   2002-2006. $T_{\delta18O}$ were calculated using Eq. (1) using a mean $\delta^{18}O_{water}$ value of -0.55 ‰. The

740   uncertainty in temperature reconstruction from $\delta^{18}O_{shell}$ is ± 0.95 °C.

741

Year	Shell	$\delta^{18}O_{shell}$ (‰VPDB)		$T_{\delta18O}$ (± 0.95°C)	
		Min.	Max.	Min.	Max.
2002	A55	2.12	3.51	1.8	7.8
	A56	2.08	3.23	3.0	8.0
2003	A55	2.06	3.29	2.8	8.1
	A56	1.93	2.92	4.4	8.7
2004	A55	2.15	3.46	2.0	7.7
	A56	1.73	3.21	3.1	9.5
2005	A55	1.64	3.05	3.8	9.9
	A56	1.96	3.45	2.1	8.5
2006	A55	-	2.92	4.4	-
	A56	-	2.98	4.1	-

742

743   Table 3. Annual minima, maxima, and amplitude of Li/Ca$_{shell}$ values of specimens A55 and

744   A56 over the period 2001-2005.

745

Year	Shell	Min. Li/Ca$_{shell}$	Max. Li/Ca$_{shell}$	Annual amplitude
2001	A55	7.26	9.40	2.13
	A56	-	-	-
2002	A55	7.29	9.29	2.01
	A56	7.64	10.42	2.77
2003	A55	7.00	9.08	2.08
	A56	7.50	10.26	2.76
2004	A55	7.08	9.39	2.32
	A56	7.10	10.03	2.92
2005	A55	7.15	9.30	2.15
	A56	7.50	11.12	3.63

746

747

748

749   **FIGURE CAPTIONS**

750

751   Fig. 1. Map of northeastern Iceland showing Langanes Peninsula between Þistilfjörður

752 and Bakkaflói. *Arctica islandica* specimens were collected by dredging in Þistilfjörður at 30

753 m water-depth (black dot). Temperature and salinity data used in this paper were measured off

754 Langanes Peninsula by the Marine Research Institute of Reykjavik (CTD station LA1, 20 m

755 water depth, black cross). Seasonality of freshwater inputs in Þistilfjörður were assessed using

756 river discharge data collected at Sandá River gauging station (black square).

757   Fig. 2. Preparation of *Arctica islandica* shells for geochemical analyses. a) Right valve

758 of *Arctica islandica*. The axis of maximum growth was identified on shells as the largest

759 distance between the umbo and the ventral margin (dashed line). b) After mounting on a

760 Plexiglas cube and embedding in metal-epoxy resin, left valves were cut along the axis of

761 maximum growth using a low-speed saw. c) Two "mirroring" sections were cut in each shell,

762 one for isotopic analyses (thick section "A") and the other one for Li/Ca determination (thick

763 section "B").

764   Fig. 3. Temporal variations (2000-2006) of Li/Ca$_{shell}$ ratio (grey circles), $\delta^{18}O_{shell}$ (black

765 triangles; inverted scale), and $\delta^{18}O_{shell}$-derived seawater temperature (T$_{\delta18O}$, grey area)

766 measured in *Arctica islandica* shells. a) Specimen A55. b) Specimen A56. Error bars on the

767 left side of each panel correspond to Li/Ca$_{min.}$ ± 1RSD, Li/Ca$_{mean}$ ± 1RSD, and Li/Ca$_{max.}$ ±

768 1RSD, with RSD = 1.9% (precision given by 22 measurements of NIST SRM 614). Vertical

769 dashed lines represent the annual growth lines revealed in shell cross-sections, and are used to

770 identify the different years of growth. Also presented are digitized cross-sections of the two

771 specimens, showing annual growth lines in outer and inner shell layers, and location of

772 aragonite samples taken for isotopic and elemental analyses.

773   Fig. 4. Correlations between $\delta^{18}O_{shell}$-derived seawater temperature ($T_{\delta18O}$) and Li/Ca$_{shell}$

774   ratio in shells A55 ($n = 48$) and A56 ($n = 50$).

775   Fig. 5. a) Li/Ca$_{shell}$ profile (grey circles) and microgrowth increment width (black

776   circles) measured during the 2004 growing season in shell A56. b) Simple linear regression

777   performed between Li/Ca$_{shell}$ and microgrowth increment width in shell A56 ($n = 22$).

778   Fig. 6. Long term smoothed daily averages of Sandá River discharge (data obtained

779   from the Hydrological Service of the Icelandic National Energy Authority). Maximum

780   discharge is recorded in May and June, i.e. in the middle of *A. islandica* shell growth season.
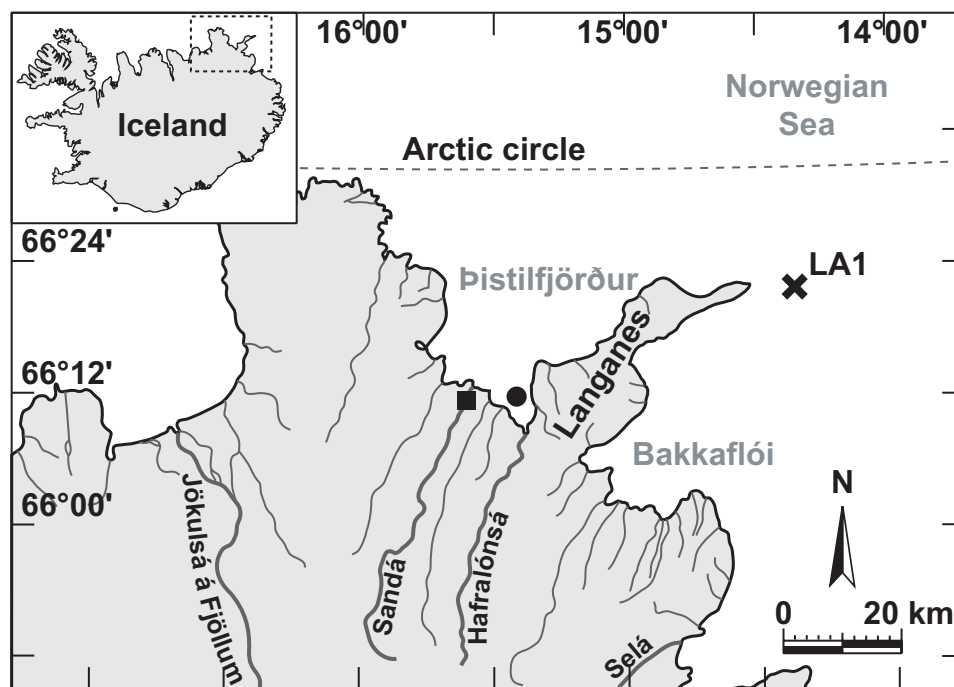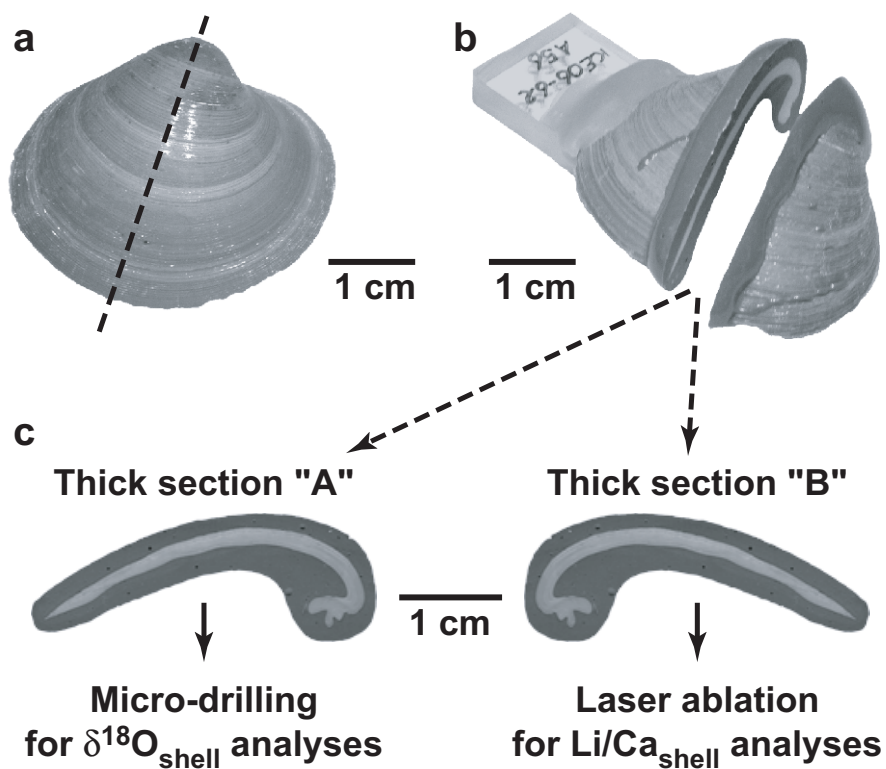
Figure 1

Figure 2
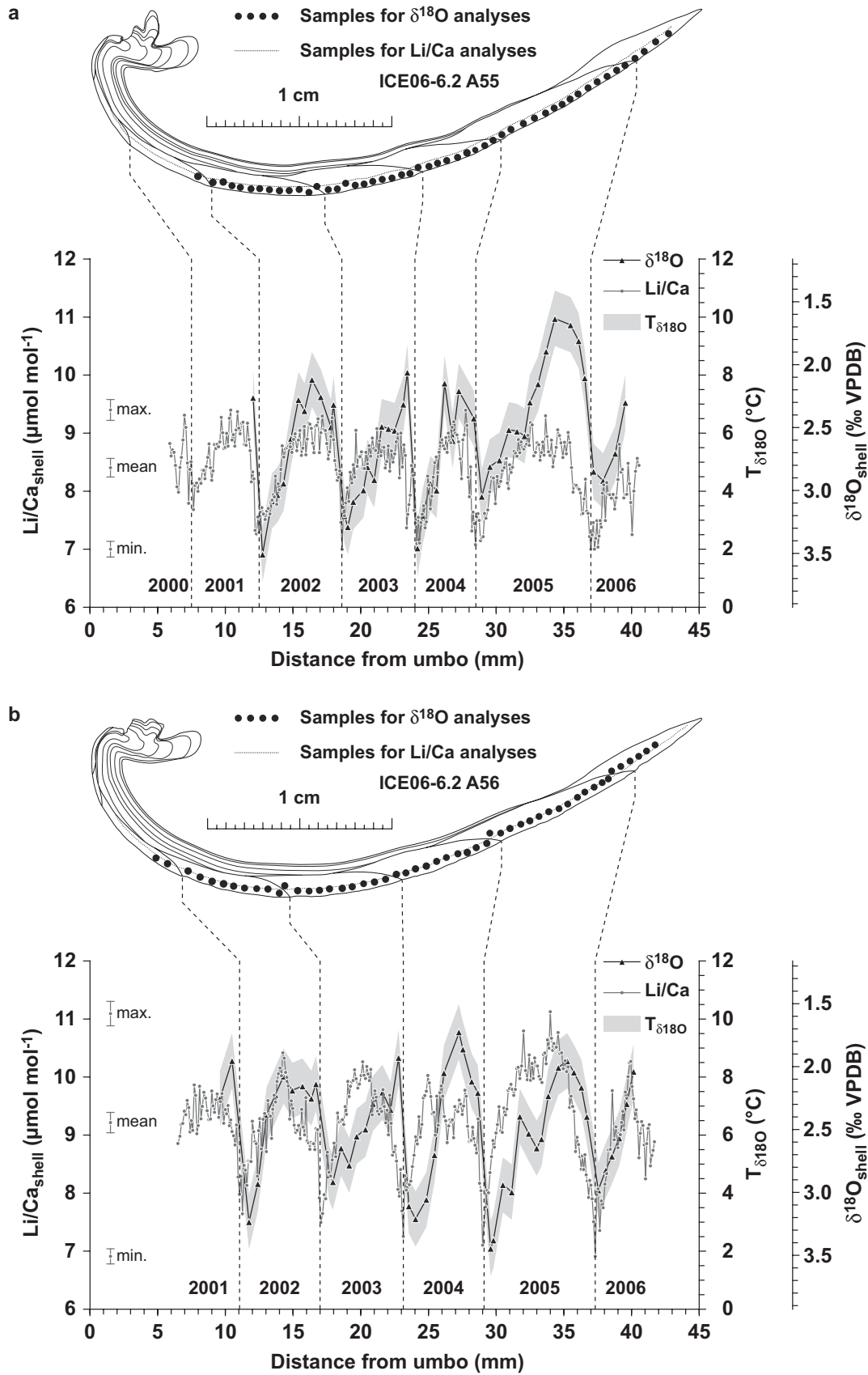

a

b

1 cm   1 cm

c

Thick section "A"

Thick section "B"

1 cm

Micro-drilling
for $\delta^{18}O_{shell}$ analyses

Laser ablation
for Li/Ca$_{shell}$ analyses

Figure 3

Figure 4

Figure 5

Figure 6